

Stress around the hole of single lapped and single bolted joint plates with fitting clearance[†]

Wenguang Liu* and Weiyan Lin

School of Aeronautical Manufacturing Engineering, Nanchang Hangkong University, Nanchang, JX 330063, China

(Manuscript Received July 5, 2018; Revised November 2, 2018; Accepted December 19, 2018)

Abstract

The effects of parameters on the stress distribution around the plate hole of a bolted joint having clearance fitting were investigated in this work. The main purpose is to reveal the interaction mechanism of different parameters and stress around a hole by theory and simulation analysis. Primarily, elastic theory was employed to derive the equilibrium equation of stress of the bolted joint plate. Subsequently, the effects of parameters, such as the bolt-hole clearance, the degree of bolt misalignment, and the pre-tightening force, on the stress around the plate hole of a bolted joint were analyzed qualitatively. Thereafter, a parametric model of single-lapped and single-bolted joint plate was created and analyzed through ABAQUS and a Python program. Finally, the effects of bolt-hole clearance, bolt misalignment, and pre-tightening force on the stress distribution around the hole were examined by case studies. Results corroborates that these parameters influence the stress magnitude around the hole and that the stress magnitude varies nonlinearly with the change in parameters. This work provides a good reference for the dynamic design of bolted joint plates.

Keywords: Fitting clearance; Stress around hole; Bolt jointed plate; Pre-tighten force

1. Introduction

Hole is one of the main potential positions of stress concentration in bolted joint structures. Cracks are commonly initiated near the bolt-hole zone of many structures due to the action of external force. If the bolted joint structure is not designed properly, then the crack will propagate, fracture, and cause great economic loss. Given that bolts are widely used in the mechanical and aerospace fields, reliability is an important concern in the aircraft design [1-3]. Many airplane crashes over the past few decades were caused by bolted joint failure [4-6]. Therefore, analysis on the magnitude of stress around a hole and its bolted structure distribution has become and will continue to be a popular issue.

During the operation of dynamic machines, bolted joint structures might be subjected to dynamic force, which allows many factors to control the stress around the bolt-hole [7-18]. Factors include the materials used in a bolted joint structure, the diameter and shape of bolts and their fitting hole, the dimension of the structure, and the variation of the pre-tightening forces. All these factors have impacts on stress magnitude and its distribution. Thus, numerous studies have been conducted on the stress around a bolt hole over the past

few decades. Lawlor et al. examined the stress distribution, quasi-static strength, failure modes, and fatigue life of a double-lapped and multi-bolted joints with different bolt-hole clearances [19]. They affirmed that the effects of bolt-hole clearance on load distribution, failure initiation load and fatigue life are significant. However, it does not affect the ultimate quasi static strength. McCarthy et al. developed a three-dimensional finite element model to study the effects of bolt-hole clearance on the mechanical behavior of a single-bolted and single-lapped joint [20]. They studied the effects of bolt-hole clearance on joint stiffness, stress state, and failure initiation. In addition, McCarthy et al. proposed a simplified method for investigating the effects of bolt-hole clearance on load distribution in a composite multi bolted joints [21]. Subsequently, both single-lapped and double-lapped bolted joints were used to validate three-dimensional finite element models with different bolt-hole clearances, and the effects of various joint parameters on load distribution were examined using this method in a case study. Gray and McCarthy provided a highly efficient modelling approach for bolted joints [22]. Shell elements were used to model the composite laminates, and the bolt was replaced by a combination of beam elements coupled with rigid contact surfaces in the strategy [23]. This method was used to study the effects of bolt-hole clearance, friction coefficient, and clamping force on the secondary and tertiary bending in the laminates and the load distribution in multi-

*Corresponding author. Tel.: +86 18079100780
E-mail address: liuwg14@nchu.edu.cn

[†]Recommended by Associate Editor Yang Zheng

© KSME & Springer 2019

bolted joints. Thereafter, they proposed an analytical method for modelling the load distribution in multi-bolt joints, and this model is a closed form extension of a spring-based method. A highly-detailed analysis of the stress distribution at the countersunk hole boundary was provided by Egan et al. [24]. They studied the clearance levels, modelled the bolt-hole clearance extensively, and validated the finite element model with experimental data. They recorded an associated loss in joint stiffness for the highest clearance. Subsequently, Egan et al. studied the mechanical performance of a joint plate with a single countersunk fastener experimentally and numerically [25]. They found the explicit dynamics method interesting due to its robust contact modelling. Gray et al. investigated problems related to the design of mechanically fastened joints in aircraft fuselage structures via experiment [26]. The effects of joint thickness, the positioning of the plies, and the secondary bending on the joint stiffness and strength were examined. A three-dimensional finite element composites composite damage model was proposed by Zhou et al. [27]. This model was applied to a problem involving highly complex, three-dimensional loadings, such as single-lapped, multi-bolted, and composite joint having variable clearances. Zhai et al. studied the effects of bolt-hole clearance and bolt clamping force on a single-lapped and single-bolted joint plate via an experimental method [28]. The bearing strength and the joint stiffness were obtained, and the effects of bolt-hole clearance and pre-tightening force on bearing response were also evaluated by varying multiple parameters. Two 3D finite element models were developed, and several tensile tests for the single-lapped bolted joint between the composite laminate and the steel with a countersunk fastener were performed by Liu et al. [29]. They showed contended that the elastic loading responses predicted by both models were consistent with the experimental results. Esmaili et al. studied the effects of clamping force on the fatigue strength of double-lap bolted joints made of 2024-T3 aluminum alloy [30]. Three sets of specimens were prepared, and fatigue tests were carried out under various cyclic axial load levels. The effects of bolt pre-tightening force on the fatigue life of double-lapped bolted joints were studied using a numerical method. Results confirmed that the estimated fatigue life was consistent with the measured fatigue life. Zhan et al. analyzed the effects of various factors on the bolted joints used in aircraft fuselage [31]. In their study, the coupled elastic plastic constitutive and fatigue damage evolution equations were derived. Esmaili et al. investigated the effects of clamping force on the fatigue life of bolted plates [32]. The available S-N curve and the notch strength reduction factor obtained from the volumetric method were employed to predict the fatigue life. Their investigation showed validated that the fatigue life of bolted plates improved because of the compressive stresses created around the plate hole due to clamping force. Chakherlou et al. studied the effects of bolt clamping force on the stress intensity and fracture strength of a plate containing a central hole with fatigue-propagated edge cracks [33]. Their results indicated asserted that the bolt

clamping force has a significant impact on reducing the stress intensity factor and the joint fracture strength. Ataş et al. presented the stress state around the hole of double-lapped and single-bolted joints under an initial clamping force [34]. They claimed that clamping force has a significant effect on composite and aluminum plates. The singular stresses arising in the neighborhood of contact surfaces in a bolted joint plate with clamping force were analyzed by Whitney et al. [35]. They proved that the characteristics of the stress singularity of the titanium bolt-head and the carbon fiber composite plate are similar to those of a crack in terms of the power of singularity and the uniqueness of the singular term. Ju examined the stress intensity factors of a bolted joint having single and double cracks [36]. Friction, bolt-hole clearance, clamping force, and crack angle were considered in the analysis, which indicated that reasonable changes in clamping force, frictional coefficient, and clearance did not result in significant changes in the normalized stress intensity factors. Toussaint et al. evaluated the mechanical response of cover-plated joints exhibiting various phenomena, such as the contact evolution between bolts and holes, the elastic-plastic behavior of the constitutive materials, and the effect of large displacements [37]. They found deduced that the complexity of stress distribution around the holes depends on the connection configurations. Hu et al. conducted an experimental study of the mechanical response of a single-lapped and single-bolted composite interference-fit joints [38]. Their results indicated inferred that the linear phase of the stress-strain behavior is prolonged by clamping force, the strain around the hole goes through a switch from the release of the residual pressure on the tensile side to the squeezing on the bearing side. Liu et al. presented an analytical method of composite single-lapped and multi-bolted joints for load distribution by using an improved three-stage method [39]. The random properties of tightening force, bolt-hole clearance, material properties, and geometric parameters were involved in the method. Samaei et al. studied the effects of clamping force on the fatigue crack growth rate and the stress intensity factors in a cracked single-lapped and simple-bolted hybrid joints. A series of fatigue tests for two different amounts of clamping force in aluminum alloy was performed to record the fatigue crack growth. Their results corroborated that a high bolt tightening torque provides improved fatigue crack growth life for both types of joints [40]. Liu and Lin investigated the effects of bolt misalignment on the stress distribution around the plate hole by simulation [41]. They affirmed that the stress concentration zone is not affected by bolt misalignment, but the peak value of the stress around the hole is related to the degree of bolt misalignment.

Although many studies have been conducted on the effects of the fitting clearance parameters on the characteristics of bolted joint, the effects of the mechanisms of fitting clearance parameters on the properties of the bolted joint remain unclear. To date, most studies were carried out by theoretical analysis, simulation calculation, and experiment. Few works have been carried out about the effects of multiple parameters on the

stress around the bolt-hole and the stress magnitude and concentration position. Again, the stress around a hole is difficult to measure not only due to the tiny space between the hole and the bolt shank, but also because many uncertainty parameters must be considered in the test. Therefore, the effects of multiple parameters on the stress around the bolt-hole must be examined to improve the reliability of bolted joints.

In the present work, a single-lapped and single-bolted joint plate was used as the study object. The analytical model of stress around the hole of the bolted joint plate was set up first based on elastic mechanics theory. The effects of the parameters on the stress around the hole were discussed qualitatively. Subsequently, a parametric finite element model of the single-bolted and single-lapped joint plate was developed using ABAQUS and a Python program. The effects of multi-parameters on the stress around the bolt-hole, both magnitude and distribution, were discussed quantitatively in the end.

2. Theoretical analysis

In this study, a single-lapped and single-bolted joint plate was considered. Fig. 1 depicts that it consists of two thin plates, a bolt, and a nut. One end of plate 1 was assumed fixed, while one end of plate 2 was subjected to a transverse external force. The lengths of plates 1 and 2 are L_1 and L_2 , respectively. The thickness of the two plates is t and their width is W . The diameter of the bolt hole in the two plates is D . The distance from the center of the bolt hole to the end of the plate is e . The two plates were assumed to be joined by the bolt with fitting clearance.

Using plate 1 as the study object, a coordinate system ($Oxyz$) was set up as shown in Fig. 2. The interface between the bolt head and plate 1 is denoted as Ω_1 . The interface between plates 1 and 2 is denoted as Ω_2 . The contact pressure stress between interfaces caused by pre-tightening force F_0 is described as $\sigma_n(x, y, z)$. The shearing stresses between interfaces caused by external force F are described as $\tau_n(x, y, z)$. The coefficients of friction between the two interfaces are defined as μ .

The pressure stress between interface Ω_1 is represented by $\sigma_n(x, y, 0)$, and the shearing stress is denoted by $\tau_n(x, y, 0)$. The pressure stress between interface Ω_2 is represented by $\sigma_n(x, y, h)$, and the shearing force is expressed as $\tau_n(x, y, h)$. According to the equilibrium condition of forces acting on plate 1, they must meet

$$\iint_{\Omega_1} \sigma_n(x, y, 0) dx dy = \iint_{\Omega_2} \sigma_n(x, y, h) dx dy = F_0 \tag{1}$$

$$\iint_{\Omega_1} \tau_n(x, y, 0) dx dy + \iint_{\Omega_2} \tau_n(x, y, h) dx dy = F \tag{2}$$

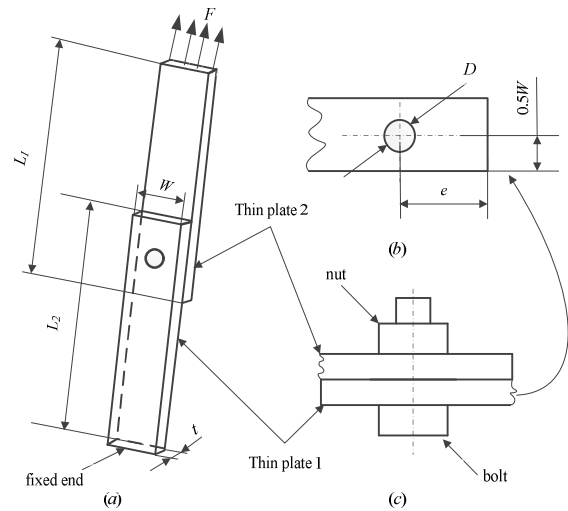


Fig. 1. Geometry model of a single-lapped and single-bolted joint plate.

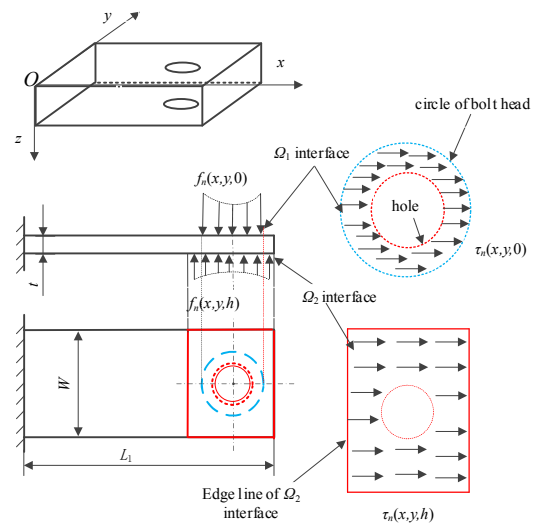


Fig. 2. Stress analysis of plate 1.

For the prevention of sliding in the interfaces of the bolt head and plate 1, plates 1 and 2, and the nut and plate 2, the frictional force of the interfaces must be larger than external force F . Thus,

$$\mu F_0 \geq F \tag{3}$$

We assumed that $\sigma_x, \sigma_y, \sigma_z, \tau_{xy}, \tau_{yz}$ and τ_{zx} were used to represent the components of stress in the bolted joint plate. Considering pressure forces $\sigma_n(x, y, 0)$ and $\sigma_n(x, y, h)$ and shearing forces $\tau_n(x, y, 0)$ and $\tau_n(x, y, h)$, the stress equation of bolted joint plate 1 in the Ω_1 and Ω_2 zones can be derived.

In zone Ω_1 , the equation is the following:

$$\frac{\partial \sigma_x(x, y, z)}{\partial x} + \frac{\partial \tau_{yz}(x, y, z)}{\partial y} + \frac{\partial \tau_{zx}(x, y, z)}{\partial z} + \tau_n(x, y, 0) = 0 \tag{4}$$

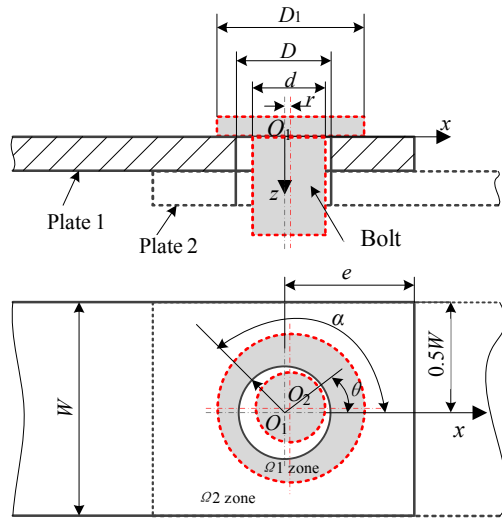


Fig. 3. Interface of Ω_1 and Ω_2 .

$$\frac{\partial \sigma_z(x, y, z)}{\partial z} + \frac{\partial \tau_{yz}(x, y, z)}{\partial x} + \frac{\partial \tau_{xz}(x, y, z)}{\partial y} + \sigma_n(x, y, 0) = 0. \tag{5}$$

In zone Ω_2 , the equation is as follows:

$$\frac{\partial \sigma_x(x, y, z)}{\partial x} + \frac{\partial \tau_{yx}(x, y, z)}{\partial y} + \frac{\partial \tau_{xz}(x, y, z)}{\partial z} + \tau_n(x, y, h) = 0, \tag{6}$$

$$\frac{\partial \sigma_z(x, y, z)}{\partial z} + \frac{\partial \tau_{zx}(x, y, z)}{\partial x} + \frac{\partial \tau_{yz}(x, y, z)}{\partial y} + \sigma_n(x, y, h) = 0. \tag{7}$$

These equations indicate that the stresses around the bolt hole of the plate are related to $\sigma_n(x, y, z)$ and $\tau_n(x, y, z)$. Pressure force $\sigma_n(x, y, z)$ and shear force $\tau_n(x, y, z)$ in plate 1 do not only depend on pre-tightening force F_0 but are also related to external force F . Furthermore, they are determined by the surface area of Ω_1 and Ω_2 zones.

Fig. 3 illustrates that the Ω_1 zone area depends on the diameters of bolt head D_1 and bolt hole D . Under the working condition, the center of the bolt might be misaligned to the center of the hole. Therefore, the Ω_1 zone area also relates to the degree of misalignment of the bolt to hole r . The Ω_2 zone area relates to the position of the hole in plates 1 and 2, implying that the zone area depends not only on the distance between e and W , but also on the diameter of the bolt hole (D).

Given the impacts of hole diameter D on the distribution of pressure force $\sigma_n(x, y, z)$ and shear force $\tau_n(x, y, z)$, the multi-parameters in Eqs. (1) and (2) can be found by testing or simulation methods. Given that the surface area of Ω_1 and Ω_2 zones affects the distribution of pressure and shear stress directly, and the Ω_1 and Ω_2 zone areas vary with the diameter of bolt

Table 1. Dimension of bolted joint plate.

L_1 (mm)	150
L_2 (mm)	150
t (mm)	3
D (mm)	6
e/D	3
W/D	3

Table 2. Material properties of aluminum.

Young's modulus E (MPa)	7.17×10^4
Poisson's ratio ν	0.33
Material density ρ (kg/m ³)	2740
Yield stress σ_s (MPa)	325
Ultimate stress σ_b (MPa)	470

hole D , the effects of bolt hole diameter D on the stress around the hole is evident. Through solving the above equations, the stress around the hole of the bolted joint plate can be analyzed qualitatively.

To clarify the effects of bolt misalignment on the stress around the hole, Fig. 3 shows that the surface area of Ω_1 and Ω_2 zones varies with the position of the bolt. The change in area due to the degree of bolt misalignment plays an important role in pressure force $\sigma_n(x, y, z)$ and shear force $\tau_n(x, y, z)$. Therefore, the interaction between the design parameters and the stress around the hole of a bolted joint plate can be determined by solving Eqs. (4)-(7). However, this is not only difficult, but it also has many requirements. In this study, a parametric finite element model was developed to examine the effects of multi-parameters on the stress around the plate hole of a bolted joint and its distribution.

3. Parametric finite element model

3.1 Model description

The dimensions of the bolted joint plate shown in Fig. 1 are provided in Table 1. The two plates are made of aluminum, while the bolt and washer are made of steel. The material properties of aluminum and steel are shown in Tables 2 and 3, respectively.

Fig. 3 shows that the center (O_1) of the top surface of plate 1 is the original point, and Ox is the polar axial. The positive direction is counterclockwise. Therefore, the position of the bolt center can be described as (r, θ) in this system. r is the offset distance and θ is the position angle of the bolt shank. It can be used to reflect the degree of bolt misalignment. Any point in the surface of the bolt hole can be described as $(D/2, \alpha, z)$. α is the position angle of point of hole surface, and z is the depth of point of hole surface. Thus, the stress of any point in the bolt-hole of the bolted joint plate could be described as $\sigma(\alpha, z)$ as D is constant.

Table 3. Material properties of steel.

Young's modulus E (MPa)	2.1×10^5
Poisson's ratio ν	0.27
Material density ρ (kg/m ³)	7850
Yield stress σ_s (MPa)	785
Ultimate stress σ_b (MPa)	980

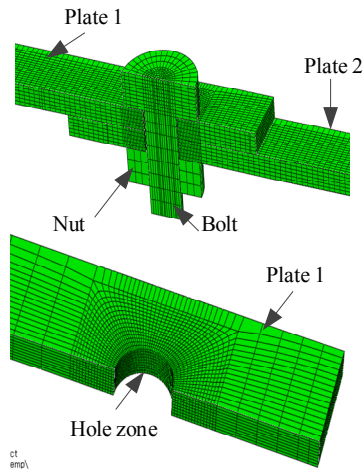


Fig. 4. Finite element model of bolted joint plate.

3.2 Finite element model

An automatically changed calculation model of the single-lapped and single-bolted joint plate with fitting clearance was developed using ABAQUS and a Python program. Fig. 4 displays the finite element model. In this model, hexahedral elements are used. Given the stress concentration around the hole due to material discontinuity, the elements near the hole zone are denser than those of the other zone.

The left end of plate 1 was fully clamped. The bolt and nut connection was modelled through the Tie method for improving the calculation efficiency because this study aims to analyze the stress around the hole both magnitude and stress distribution. For the investigation of the effects of pre-tightening force on the stress around the hole, different pre-tightening forces F_0 were applied to the bolted joint to prevent the relative sliding between plates 1 and 2 when they are subjected to external force F . The contact surfaces between plates 1 and 2, the bolt head and plate 1, and the nut and plate 2 were defined as hard contact, and the penalty coefficient was set to 0.15. A uniform pressure was applied to the free end of plate 2, that is, 0.1 MPa to represent force F .

3.3 Procedure of stress analysis

During the calculation of the stress around the bolt hole, the parametric finite element model of a single-lapped and single-bolted joint plate with different parameters was created automatically using ABAQUS and a Python program. With these finite element models, the stress around the bolt hole was ana-

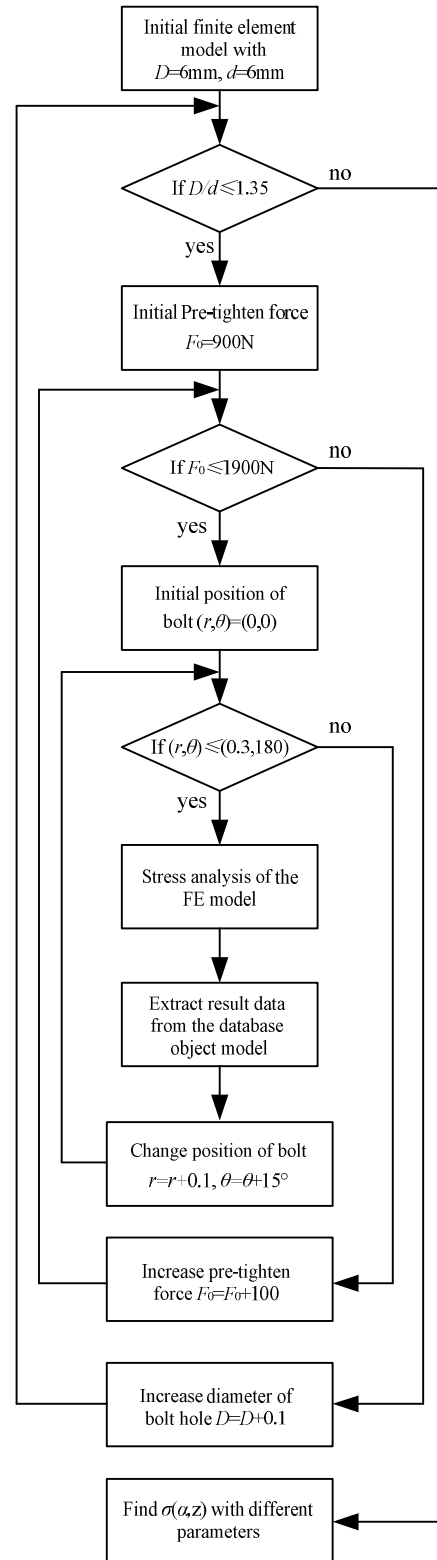


Fig. 5. Flowchart of stress analysis.

lyzed. Data were extracted from the database object model. The diameter of bolt shank d was set to 6 mm. The step length of α was 6° . Fig. 5 shows the flowchart of the stress analysis

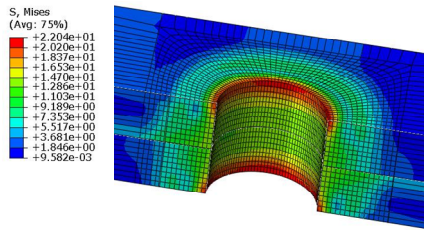


Fig. 6. Stress contour around the hole.

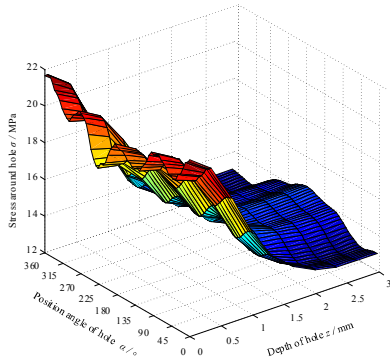


Fig. 7. Stress distribution around the plate hole.

around the plate hole of the bolted joint.

4. Results and discussion

4.1 Stress distribution around hole

Fig. 6 examines the stress contour around the hole when pre-tightening force $F_0 = 1000\text{ N}$ was applied to the bolt. Results contend that the von-mises stress around the hole between the bolt head and plate 1 and that between nut and plate 1 is bigger than the stress of other places. The maximum stress is approximately 22 MPa.

Fig. 7 shows the relation of stress magnitude around the hole and the depth of the hole. The concentration position of stress around the hole is mainly distributed at the position of $\alpha = 0^\circ, 90^\circ, 180^\circ, 270^\circ$. With the increase of the depth of the bolt hole, the stress magnitude around the hole decreases. When the depth of the hole is between 0 mm and 1.5 mm, the stress magnitude around the bolt-hole decreases linearly with the depth of the hole. However, as the depth of the hole is between 1.5 mm and 3.0 mm, the effects of the depth of the hole on stress magnitude can be neglected.

4.2 Effects of bolt-hole clearance on stress around the hole

Figs. 8-10 show the relation of stress around the hole with different bolt-hole clearances when pre-tighten force F_0 is set to 1000 N and (r, θ) to $(0, 0)$.

Results validate that the stress around the hole decreases with the increase of the diameter ratio (D/d). As diameter ratio D/d increases by 25 %, the magnitude of stress decreases by nearly 45 %. The law of stress distribution as the depth of the hole of $z = 1.5\text{ mm}$ is similar with that of $z = 0\text{ mm}$. However,

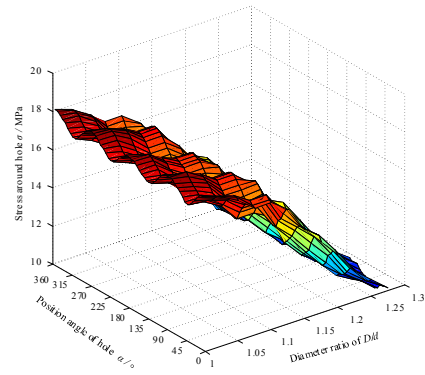


Fig. 8. Effects of bolt-hole clearance on stress around the hole when $z = 0\text{ mm}$.

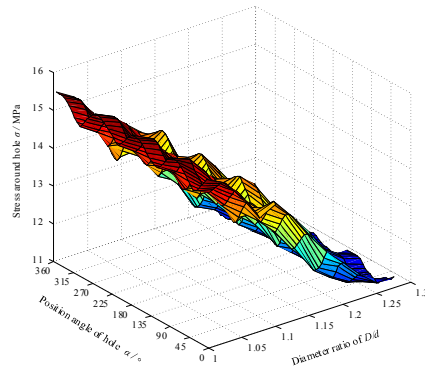


Fig. 9. Effects of bolt-hole clearance on stress magnitude around the hole when $z = 1.5\text{ mm}$.

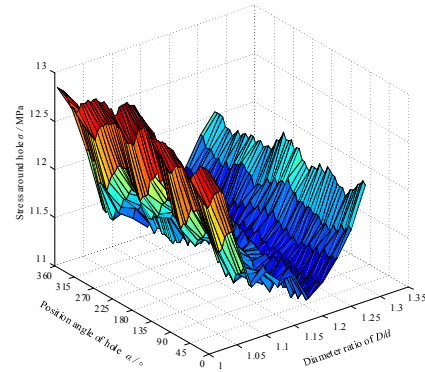


Fig. 10. Effects of bolt-hole clearance on stress magnitude around the hole when $z = 3.0\text{ mm}$.

as the magnitude of stress around the bolt-hole decreases to 30 % as diameter ratio D/d increases 25 %, when $z = 3\text{ mm}$, the magnitude of stress around the bolt-hole decreases with the increasing D/d when it is between 1 and 1.1. When D/d is between 1.1 and 1.2, the increase in diameter of the bolt-hole has no effect on the stress magnitude around the hole. When D/d is between 1.2 and 1.3, the stress around the bolt-hole increases with the diameter of the bolt-hole.

To understand the relation of diameter ratio D/d and the stress around the hole, Fig. 11 shows the change law of stress with D/d . As D/d is between 1 and 1.23, the magnitude of

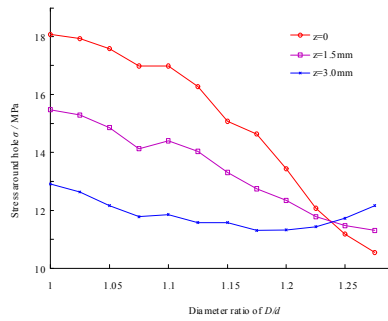


Fig. 11. Stress magnitude vs. diameter ratio.

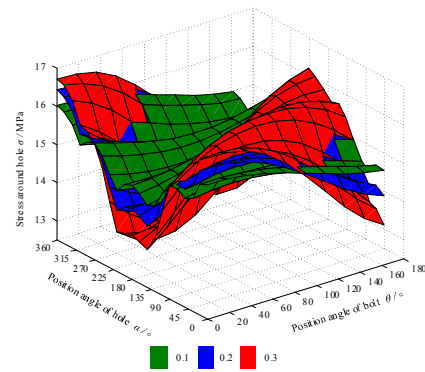


Fig. 13. Effects of misalignment on stress around the hole as $z = 1.5$ mm.

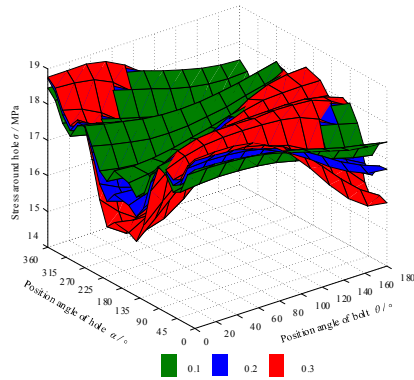


Fig. 12. Effects of misalignment on stress around the hole when $z = 0$ mm.

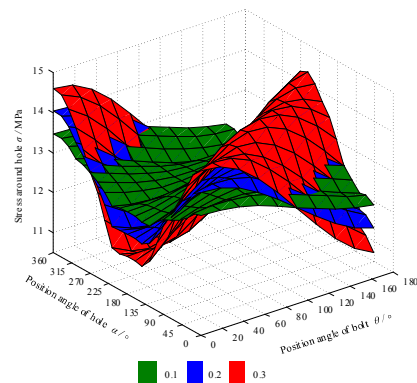


Fig. 14. Effects of misalignment on stress around the hole when $z = 3.0$ mm.

stress around the hole decreases with the increase of the depth of z when $\alpha = 90^\circ$. However, when D/d is larger than 1.23, the magnitude of stress around the hole decreases with the increase of the depth of z when $\alpha = 90^\circ$. Especially, when D/d equals to 1.23, the stress magnitude is the same when $z = 0$ mm, 1.5 mm, 3 mm. This property is very helpful in the design of bolted joint structures.

4.3 Effects of misalignment on stress around hole

Figs. 12-14 investigate the effects of the degree of bolt and hole misalignment on the stress around the hole when pre-tightening force $F_0 = 1000$ N. In these figures, the response surfaces in green represents $r = 0.1$ mm, blue represents $r = 0.2$ mm, and red represents $r = 0.3$ mm. Results verify that the relation of stress around the bolt-hole and the degree of bolt misalignment under different offset distances are very similar. In addition, the stress magnitude around the bolt hole decreases with the increasing hole depth. The stress magnitude is the maximum value when $z = 0$ mm, the minimum when $z = 3$ mm. The stress magnitude is proportional to the nearness of the bolt center to the center of the bolt hole.

Fig. 15 shows the relation of stress magnitude and the degree of bolt and hole misalignment. When θ is between 0 and 180° , the maximum stress appears at $\theta = 90^\circ$, but the minimum stress appears at $\theta = 0^\circ$ and $\theta = 180^\circ$, which implies that installing the bolt at $(r, 0^\circ)$ and $(r, 180^\circ)$ is helpful in reducing

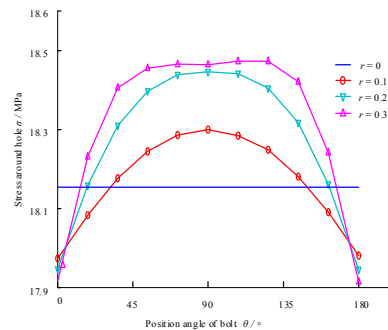


Fig. 15. Amplitude of stress vs. degree of misalignment.

the stress amplitude when $\alpha = 90^\circ$. This conclusion is helpful in improving the fatigue strength of bolted joint structures. The larger r is, the better its effect is.

4.4 Effect of pre-tighten force on stress

Figs. 16-18 illustrate the effects of pre-tightening force on the stress magnitude around the bolt-hole as the pre-tightening force is set from 900 N to 1900 N.

Results assert that the stress magnitude around the hole increases linearly with the pre-tightening force. When the depth of the hole is $z = 0$ mm, the maximum stress magnitude

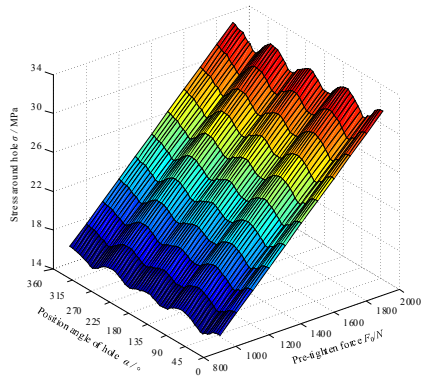


Fig. 16. Effects of pre-tightening force on stress magnitude when $z = 0$.

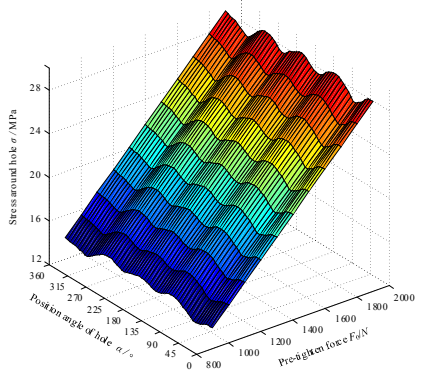


Fig. 17. Effects of pre-tightening force on stress magnitude when $z = 1.5$ mm.

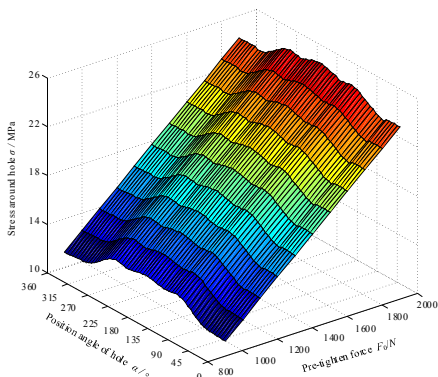


Fig. 18. Effects of pre-tightening force on stress magnitude when $z = 3.0$ mm.

around the hole reaches 34 MPa, and is 24 MPa when $z = 3$ mm. Under a certain pre-tightening force, the maximum stress is achieved when $\alpha = 0^\circ, 90^\circ, 180^\circ, 270^\circ$. Fig. 19 shows the relation of stress around the hole and pre-tightening force. Results claim that the magnitude of stress increases with the pre-tightening force.

Although an analytical method was proposed for analyzing the stress around the bolt hole of a bolted joint with multi-parameters in this study, the stress around the hole was not verified by experimental result. Thus, our future research will be focused on monitoring the stress around the bolt hole.

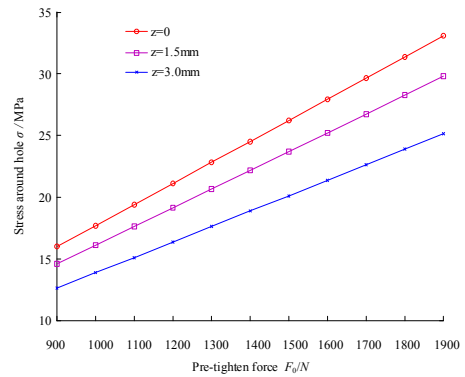


Fig. 19. Amplitude of stress vs. pre-tightening force.

5. Conclusions

The stress equation of a bolted joint plate was set up mathematically and the effects of parameters on the stress around the bolt hole are analyzed qualitatively. A parametric finite element model of the single-lapped and single-bolted joint plate was developed by ABAQUS. Finally, the effects of the diameter ratio of the bolt-hole to the bolt shank, the degree of bolt misalignment, and the pre-tightening force on the stress around the hole were analyzed quantitatively. The following main conclusions are drawn:

(1) The position angles of the hole $\alpha = 0^\circ, 90^\circ, 180^\circ, 270^\circ$ are the main positions of stress concentration. The stress magnitude around the bolt-hole decreases with the depth of hole linearly when z is between 0 mm and 1.5 mm. However, the depth of the hole has no effect on stress when z is between 1.5 mm and 3.0 mm.

(2) The magnitude of stress around the hole decreases with the increase in depth of z when $\alpha = 90^\circ$ and D/d is between and 1.23. However, the magnitude of stress around the hole decreases with the increase of the depth of z when $\alpha = 90^\circ$ and D/d is larger than 1.23. The stress magnitude is the same when $z = 0, 1.5$ and 3 mm.

(3) The stress magnitude is proportional to the nearness of the bolt center to the center of the bolt hole. The maximum stress appears at $\theta = 90^\circ$, but the minimum stress appears at $\theta = 0^\circ$ and $\theta = 180^\circ$.

(4) The stress around the hole increases linearly with the pre-tightening force. The maximum stress is achieved when $\alpha = 0^\circ, 90^\circ, 180^\circ, 270^\circ$ under a certain pre-tightening force.

Acknowledgments

This research work is supported by the National Natural Science Foundation of China (51565039) and the Jiangxi Provincial Natural Science Foundation (20181BAB206023).

Nomenclature

- d : Diameter of bolt shank
- D : Diameter of hole
- D_1 : Diameter of bolt head

e	: Distance from hole center to the end of plate
E	: Elastic modulus of material
F	: External force
F_0	: Pre-tighten force
L_i	: Length of plate 1 and plate 2 ($i=1,2$)
t	: Thickness of plate
r	: Offset distance of bolt position
W	: Width of plate
Ω_1	: Interface between bolt head and plate 1
Ω_2	: Interface between plate 1 and plate 2
ρ	: Material density
ν	: Poisson's ratio
σ_n	: Contact pressure stress
μ	: Lateral deflection in z direction of the right beam
τ_n	: Shearing stress
θ	: Position angle of bolt shank
α	: Position angle of point of hole surface

References

- [1] F. Adel, S. Shokrollahi, M. Jamal-Omidi and A. Ahmadian, A model updating method for hybrid composite/aluminum bolted joints using modal test data, *J. of Sound and Vibration*, 396 (2017) 172-185.
- [2] P. Lopez-Cruz, J. Laliberté and L. Lessard, Investigation of bolted/bonded composite joint behaviour using design of experiments, *Composite Structures*, 170 (2017) 192-201.
- [3] Y. Cao, Z. Cao, Y. Zuo, L. Huo, J. Qiu and D. Zuo, Numerical and experimental investigation of fitting tolerance effects on damage and failure of CFRP/Ti double-lap single-bolt joints, *Aerospace Science and Technology*, 78 (2018) 461-470.
- [4] Y. Wang, J. Wu, H. Liu, K. Kuang, X. Cui and L. Han, Analysis of elastic interaction stiffness and its effect on bolt preloading, *International J. of Mechanical Sciences*, 130 (2017) 307-314.
- [5] B. Zhang, C. Tao and C. Liu, Cracking analysis on joint lug of aluminum alloy framework of an airplane, *Engineering Failure Analysis*, 35 (2013) 82-87.
- [6] D. J. Benac, Technical brief: Avoiding bolt failures, *J. of Failure Analysis and Prevention*, 7 (2) (2007) 79-80.
- [7] N. M. Chowdhury, J. Wang, W. K. Chiu and P. Chang, Static and fatigue testing bolted, bonded and hybrid step lap joints of thick carbon fibre/epoxy laminates used on aircraft structures, *Composite Structures*, 142 (2016) 96-106.
- [8] J. M. Mínguez and J. Vogwell, Effect of torque tightening on the fatigue strength of bolted joints, *Engineering Failure Analysis*, 13 (8) (2006) 1410-1421.
- [9] C. Santiuste, E. Barbero and M. H. Miguelez, Computational analysis of temperature effect in composite bolted joints for aeronautical applications, *J. of Reinforced Plastics and Composites*, 30 (1) (2011) 3-11.
- [10] F. Iancu, X. Ding, G. L. Cloud and B. B. Raju, Three-dimensional investigation of thick single-lap bolted joints, *Experimental Mechanics*, 45 (4) (2005) 351-358.
- [11] M. Keikhosravy, R. H. Oskouei, P. Soltani, A. Atas and C. Soutis, Effect of geometric parameters on the stress distribution in Al 2024-T3 single-lap bolted joints, *International J. of Structural Integrity*, 3 (1) (2012) 79-93.
- [12] M. Pau, A. Baldi and B. Leban, Visualization of contact areas in bolted joints using ultrasonic waves, *Experimental Techniques*, 32 (4) (2010) 49-53.
- [13] J. P. Kabche, V. Caccese, K. A. Berube and R. Bragg, Experimental characterization of hybrid composite-to-metal bolted joints under flexural loading, *Composites Part B: Engineering*, 38 (1) (2007) 66-78.
- [14] J. Wang, B. Uy, H. T. Thai and D. Li, Behaviour and design of demountable beam-to-column composite bolted joints with extended end-plates, *J. of Constructional Steel Research*, 144 (2018) 221-235.
- [15] E. Cavène, S. Durif, A. Bouchaïr and E. Toussaint, Experimental study of cover-plate bolted joints with large or slotted holes, *Ce/papers*, 1 (2-3) (2017) 272-281.
- [16] L. V. Awadhani and A. Bewoor, Parametric study of composite bolted joint under compressive loading, *Procedia Manufacturing*, 22 (2018) 186-195.
- [17] J. Armand, L. Salles, C. W. Schwingshack, D. Süß and K. Willner, On the effects of roughness on the nonlinear dynamics of a bolted joint: A multiscale analysis, *European J. of Mechanics - A/Solids*, 70 (2018) 44-57.
- [18] M. Sanati, Y. Terashima, E. Shamoto and S. S. Park, Development of a new method for joint damping identification in a bolted lap joint, *J. of Mechanical Science and Technology*, 32 (5) (2018) 1975-1983.
- [19] V. P. Lawlor, M. A. McCarthy and W. F. Stanley, An experimental study of bolt-hole clearance effects in double-lap, multi-bolt composite joints, *Composite Structures*, 71 (2) (2005) 176-190.
- [20] M. A. McCarthy, C. T. McCarthy, V. P. Lawlor and W. F. Stanley, Three-dimensional finite element analysis of single-bolt, single-lap composite bolted joints: Part I-model development and validation, *Composite Structures*, 71 (2) (2005) 140-158.
- [21] M. A. McCarthy, C. T. McCarthy and G.S. Padhi, A simple method for determining the effects of bolt-hole clearance on load distribution in single-column multi-bolt composite joints, *Composite Structures*, 73 (1) (2006) 78-87.
- [22] P. J. Gray and C. T. McCarthy, A global bolted joint model for finite element analysis of load distributions in multi-bolt composite joints, *Composites: Part B*, 41 (4) (2010) 317-325.
- [23] C. T. McCarthy and P. J. Gray, An analytical model for the prediction of load distribution in highly torqued multi-bolt composite joints, *Composite Structures*, 93 (2) (2011) 287-298.
- [24] B. Egan, C. T. McCarthy, M. A. McCarthy and R. M. Frizzell, Stress analysis of single-bolt, single-lap, countersunk composite joints with variable bolt-hole clearance, *Composite Structures*, 94 (3) (2012) 1038-1051.
- [25] B. Egan, C. T. McCarthy, M. A. McCarthy, P. J. Gray and R. M. Frizzell, Modelling a single-bolt countersunk compos-

- ite joint using implicit and explicit finite element analysis, *Computational Materials Science*, 64 (2012) 203-208.
- [26] P. J. Gray, R. M. O'Higgins and C. T. McCarthy, Effect of thickness and laminate taper on the stiffness, strength and secondary bending of single-lap, single-bolt countersunk composite joints, *Composite Structures*, 107 (2012) 315-324.
- [27] Y. Zhou, H. Y. Nezhad, C. Hou, X. Wan and C. T. McCarthy, A three dimensional implicit finite element damage model and its application to single-lap multi-bolt composite joints with variable clearance, *Composite Structures*, 131 (2015) 1060-1072.
- [28] Y. Zhai, D. Li, X. Li, L. Wang and Y. Yin, An experimental study on the effect of bolt-hole clearance and bolt torque on single-lap, countersunk composite joints, *Composite Structures*, 127 (2015) 411-419.
- [29] P. Liu, X. Cheng, S. Wang, S. Liu and Y. Cheng, Numerical analysis of bearing failure in countersunk composite joints using 3D explicit simulation method, *Composite Structures*, 138 (2016) 30-39.
- [30] F. Esmaili, T. N. Chakherlou and M. Zehsaz, Investigation of bolt clamping force on the fatigue life of double lap simple bolted and hybrid (bolted/bonded) joints via experimental and numerical analysis, *Engineering Failure Analysis*, 45 (2014) 406-420.
- [31] Z. Zhan, Q. Meng, W. Hu, Y. Sun, F. Shen and Y. Zhang, Continuum damage mechanics based approach to study the effects of the scarf angle, surface friction and clamping force over the fatigue life of scarf bolted joints, *International J. of Fatigue*, 102 (2017) 59-78.
- [32] F. Esmaili, T. N. Chakherlou, M. Zehsaz and S. Hasani-fard, Investigating the effect of clamping force on the fatigue life of bolted plates using volumetric approach, *J. of Mechanical Science and Technology*, 27 (12) (2013) 3657-3664.
- [33] T. N. Chakherlou, B. Abazadeh and J. Vogwell, The effect of bolt clamping force on the fracture strength and the stress intensity factor of a plate containing a fastener hole with edge cracks, *Engineering Failure Analysis*, 16 (1) (2009) 242-253.
- [34] A. Ataş, C. Soutis and N. Arslan, A qualitative comparison of stresses at aircraft bolted joint holes under initial clamping force, *Procedia Engineering*, 10 (2011) 3-8.
- [35] T. J. Whitney, E. V. Iarve and R. A. Brockman, Singular stress fields near contact boundaries in a composite bolted joint, *International J. of Solids and Structures*, 41 (7) (2004) 1893-1909.
- [36] S. H. Ju, Stress intensity factors for cracks in bolted joints, *International J. of Fracture*, 84 (2) (1997) 129-141.
- [37] E. Toussaint, S. Durif, A. Bouchaïr and M. Grédiac, Strain measurements and analyses around the bolt holes of structural steel plate connections using full-field measurements, *Engineering Structures*, 131 (2017) 148-162.
- [38] J. Hu, K. Zhang, Q. Yang, H. Cheng, P. Liu and Y. Yang, An experimental study on mechanical response of single-lap bolted CFRP composite interference-fit joints, *Composite Structures*, 196 (2018) 76-88.
- [39] F. Liu, M. Shan, L. Zhao and J. Zhang, Probabilistic bolt load distribution analysis of composite single-lap multi-bolt joints considering random bolt-hole clearances and tightening torques, *Composite Structures*, 194 (2018) 12-20.
- [40] M. Samaei, M. Zehsaz and T. N. Chakherlou, Experimental and numerical study of fatigue crack growth of aluminum alloy 2024-T3 single lap simple bolted and hybrid (adhesive/bolted) joints, *Engineering Failure Analysis*, 59 (2016) 253-268.
- [41] W. Liu and W. Lin, Effects of bolt misalignment on stress around plate hole, *International Conference on Mechanical Design*, Springer, Singapore (2017) 1511-1524.



Wenguang Liu received his Ph.D. degree from Nanjing University of Aeronautics and Astronautics, China. He is currently working as Associate Professor in Nanchang Hangkong University, China.